



Eco-friendly rice husk pre-treatment for preparing biogenic silica: Gluconic acid and citric acid comparative study

Wahyu Kamal Setiawan, Kung-Yuh Chiang*

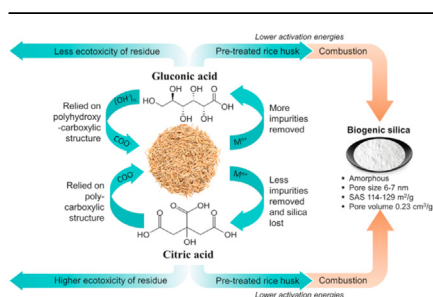
Graduate Institute of Environmental Engineering, National Central University, No. 300, Chung-Da Road., Chung-Li District, Tao-Yuan City, 32001, Taiwan



HIGHLIGHTS

- A comparative study of GA and CA leaching in BSi preparation was conducted.
- GA leaching exhibited higher efficiency than CA leaching on the BSi recovery.
- Both GA and CA leaching enhanced RH thermal degradation.
- Both GA and CA produced high-purity BSi with identical properties.
- GA leaching was environmentally better than CA leaching.

GRAPHICAL ABSTRACT



ARTICLE INFO

Article history:

Received 11 December 2020
 Received in revised form
 27 March 2021
 Accepted 6 April 2021
 Available online 9 April 2021

Handling Editor: Derek Muir

Keywords:

Gluconic acid
 Citric acid
 Rice husk
 Biogenic silica

ABSTRACT

Carboxylic acid leaching has been established eco-friendly pre-treatment method for producing biogenic silica (BSi) from rice husk. The most urgent issue is for carboxylic acid to promote new readily biodegradable acids and enhance carboxylic acid sustainability in BSi preparation. This research investigates gluconic acid (GA) applicability for biogenic silica preparation from rice husk compared with citric acid (CA). The results demonstrated that GA was preferable to CA on BSi recovery with 89.91% efficiency. Although GA leaching promoted slightly higher silica loss, the primary metal alkali impurities, such as K_2O , Na_2O , and Al_2O_3 , were effectively removed at 92–93%, 89–93%, 95–97%, respectively. The combination effect of silica loss and high removal impurities resulted in lower rice husk thermal decomposition activation energy. The characteristics of BSi prepared by GA leaching were comparable with CA leaching, mainly mesoporous with $114.06 \text{ m}^2/\text{g}$ of specific surface area and $0.23 \text{ cm}^3/\text{g}$ of the pore volume. In addition, GA leaching was environmentally better than CA leaching, indicated by minor contribution to all environmental impact indices. The findings suggested that GA could be a potential replacement for prevalent carboxylic acids in BSi preparation.

© 2021 Published by Elsevier Ltd.

1. Introduction

Rice husk (RH) is one of the most plentiful agricultural residues in the world. It is rich in organic matters (e.g., cellulose,

hemicellulose, and lignin) with a typical high ash content characteristic (Su et al., 2020). Highly organic compounds in RH could be applied to generate biofuels (briquettes, biogas, bio-oil) through the thermochemical process, adsorbents for environmental control (biochar and activated carbon), and construction materials (natural fibers) (Goodman, 2020). The RH ash is mainly composed of SiO_2 with trace amounts of alkali (e.g. Na, K), alkaline (e.g. Ca, Mg), transition metals (e.g. Al, Fe, Cu, Zn), and non-metals (e.g. Cl, S, P)

* Corresponding author. Graduate Institute of Environmental Engineering, National Central University, Tao-Yuan City, 32001, Taiwan.
 E-mail address: kychiang@ncu.edu.tw (K.-Y. Chiang).

(Zhang et al., 2018). Consequently, it can be identified as a high-prospect crop residue for biogenic silica (BSi) valorization (Setiawan and Chiang, 2020). BSi produced from RH is a renewable precursor for developing silica derivative products such as concrete materials (Gomes et al., 2020), refractory ceramic materials (Mathur et al., 2018), composite materials (Jyoti et al., 2021), additive materials for epoxy resin (Pham et al., 2017; Bach et al., 2019; Vu et al., 2020a, 2020b), adsorbents for pollutant removal (Pham et al., 2020a, 2020b), catalysts materials (Davarpanah et al., 2019), or even chemotherapeutic agents (Dhinasekaran et al., 2020). Therefore, to develop eco-friendly pre-treatment techniques for preparing BSi have begun to pay more attention to by many researchers.

Combining pre-treatment strategies with a combustion process can be applied to produce high-quality BSi from RH (Beidaghy Dizaji et al., 2019). RH pre-treatment is a critical step in removing non-siliceous components before oxidizing organic fractions through the thermal process. That was regarded for the following reasons. The alkali elements (e.g., Na and K) and silicate species create eutectic reactions during the combustion process to form ternary oxides. This reaction is responsible for decreasing the melting-point of silicate species to around 800 °C, which results in the amorphous silica crystallization nature. Because of that, the carbon originated from RH organics can easily be dissolved into ternary oxides, accelerating the formation of black particles (Chen et al., 2017). It also promotes slagging and fouling on heat transfer surfaces, threatening safe operation and increasing the operating cost.

Among all pre-treatment technologies, acid leaching has been approved to be practical and highly efficient (Duan et al., 2018). Leaching processes with inorganic acids such as HCl, H₂SO₄, and HNO₃ are widely used to remove metal alkali components during BSi production (Bakar et al., 2016; Chen et al., 2017; Xu et al., 2018). The application of these strong acids ensures the exceptional high purity and amorphous structure of BSi. However, it has extensive economic and environmental restrictions regarding the utilization of inexpensive chemicals with hazardous residues, corrosion problems, and particular disposal treatment (Alyosef et al., 2013). The replacement of such strong acids with new eco-friendly ones is highly recommended to undertake the above-mentioned drawbacks. The lower molecular weight of organic acids, such as citric acid (Schneider et al., 2020), acetic acid (Chen et al., 2017), and oxalic acid (Lee et al., 2017), have been reported as good alternatives throughout the RH leaching process to produce BSi.

Citric acid, C₆H₈O₇ (CA), has received significant attention as an organic acid for preparing BSi from RH. It was related to the outstanding ability to form a complex with numerous metallic ions (Karwowska, 2012; Xia et al., 2015; Martínez et al., 2018). Indeed, the high purity of BSi, up to 99.77%, has been successfully obtained by employing CA RH leaching before the combustion process (Umeda and Kondoh, 2010). Nevertheless, the high global demand for CA in food and beverages (70%) could probably be a solemn impediment for developing CA as a leaching agent in BSi production. Purchasing CA is also troublesome due to the high cost of raw materials and energy (Vandenbergh et al., 2017). Accordingly, the CA price was estimated at 0.73–0.95 \$/kg (Wang et al., 2020). Therefore, prospecting other non-toxic, harmless, and biodegradable acids is beneficial to encourage widespread green processing in BSi production from crop residues.

Gluconic acid, C₆H₁₂O₇ (GA), indeed, will be noteworthy for investigation in carboxylic acid leaching regarding its excellent performance to chelate di- and trivalent metal ions such as Al³⁺, Ca²⁺, Fe³⁺, and Zn²⁺ (Cañete-Rodríguez et al., 2016; Pal et al., 2016). Likewise, its biodegradability is remarkable (98% for 48 h

(Ramachandran et al., 2006). Even though the GA market is comparatively smaller than that for CA, its increasing demand in different industries has sparked concerns in developing GA economic production (Pal et al., 2016). At present, GA production is estimated at around 100,000 tons/year and commercially available as a 50% technical grade aqueous solution (by mass) (Cañete-Rodríguez et al., 2016). The production cost of GA through novel eco-friendly technologies (e.g., electrodialysis and bipolar membrane electro dialysis) was relatively affordable at 0.067–0.25 \$/kg (Lei et al., 2020).

Therefore, the innovative points and objectives of this study are (1) to investigate the applicability of GA for preparing BSi from RH compared to CA; (2) to characterize the performances of GA leaching efficiency on metal alkali species; (3) to assess the impacts on the thermal degradation behavior of RH and the characteristics of BSi; (4) to evaluate potential environmental effects of GA and CA application in the leaching process by life cycle assessment (LCA). The results will provide insights on GA potential as an eco-friendly leaching process for extracting crop residues-derived silica.

2. Material and methods

2.1. Materials

The RH samples used in this research were obtained from Lianfu Rice Mill, located in Taoyuan City, Taiwan. The primary raw RH sample properties are provided in Table 1. Proximate analysis, including moisture, ash content, volatile matter, and fixed carbon, were determined in triplicate using regulated testing procedures of the Taiwan Environmental Protection Administration (EPA) (NIEA R213 and R205) and the Chinese National Standard (CNS 10823). The ultimate analysis of RH was also measured by an elemental analyzer (Elementary Analyzer, Vario MICRO). The energy content of the RH was determined using a bomb calorimeter (Parr 1341

Table 1
Basic properties of raw RH sample.

Characteristics	Value
<i>Proximate analysis (wt.%, as received)</i>	
Moisture	10.11 ± 0.18
Ash	18.85 ± 1.55
Volatile matter	53.75 ± 2.11
Fixed carbon ^a	17.29
<i>Ultimate analysis (wt.%, wet basis)</i>	
C	34.53 ± 0.47
H	4.61 ± 0.10
N	0.39 ± 0.07
S	0.12 ± 0.01
Cl	0.28 ± 0.02
O ^b	31.12
<i>Energy content (kcal/kg)</i>	
Higher heating value	3362 ± 184.69
Lower heating value	3053
<i>Elemental composition of ash (wt.%, dry based)</i>	
SiO ₂	91.60 ± 0.03
Al ₂ O ₃	2.21 ± 0.02
Fe ₂ O ₃	0.28 ± 0.02
MnO	0.17 ± 0.00
CuO	0.03 ± 0.00
ZnO	0.02 ± 0.00
CaO	1.02 ± 0.01
K ₂ O	3.34 ± 0.01
Na ₂ O	0.85 ± 0.01
MgO	0.47 ± 0.00

^a By difference (Fixed carbon% = 100%-Moisture%-Ash%-Volatile matter %).

^b By difference (O% = 100%- Moisture%-Ash%-C%-H%-N%-S%-O%-Cl %).

calorimeter) (NIEA E214.01C). Citric acid monohydrate with 99.9% purity (CAS-No.5949-29-1) was purchased from Avantor Performance Materials Inc (Radnor, PA, United States). D-gluconic acid, 50% aqueous solution (CAS-No.526-95-4), was acquired from Alfa Aesar (Haverhill, MA, United States). To further understand the CA and GA leaching performances, chemical characteristics and structures of CA and GA are indicated in Table S1 and Fig. 1.

2.2. Carboxylic acid leaching and BSi generation

The carboxylic acid leaching was carried out following the previously reported procedures (Umeda and Kondoh, 2010). Thirty grams of RH samples were respectively immersed in 500 ml acid solutions and heated at 80 °C for 2 h under vigorous stirring. The CA and GA concentrations ranged from 0, 0.05, 0.15, 0.25, 0.35 mol/L. A microprocessor pH meter (SUNTEX SP-2200) was used to measure pH solutions. The treated RH was then filtered out from the leaching solutions and washed using deionized water under vigorous stirring. Consequently, it was dried and combusted at 800 °C for 2 h to obtain BSi.

Leaching efficiency was determined using the following equation below:

$$\text{Efficiency (\%)} : \left| \left(\frac{X_f}{X_i} \right) - \left(\frac{Y_f}{Y_i} \right) \right| \times 100\% \quad (1)$$

X_f and Y_f are the final amounts of silica and impurities remaining in the final product. X_i and Y_i represent the initial amounts of silica and impurities in RH, respectively.

In this research, the leaching efficiency of BSi could be evaluated in terms of recovered Si percentages and Si purity. Recovered Si percentage can be determined by calculating the weight ratio between the residual silica in RH after leaching process (X_f) and the initial silica amount in RH (X_i) (as indicated in Eq. (1)). That is, the recovered silica refers to the amount of silica that is not to be dissolved into water or aqueous solution. Silica purity is used to describe the leaching performance. The BSi purity represents the silica quality in terms of its contamination by the other chemical compositions. In other words, the impurity percentage of BSi can be defined in this research as Y_f/Y_i in Eq. (1). Therefore, leaching efficiency values are essential to evaluate the best carboxylic acid leaching performance. The good leaching efficiency could represent the high recovery and low impurity of BSi produced from RH by carboxylic acid leaching.

2.3. Thermal kinetic analysis

Thermal decomposition behavior of treated and un-treated rice RH was carried out using a thermal analyzer integrated with heat flux type DTA and TGA unit (HITACHI TG/DTA 7300). Approximately 9.50 ± 0.1 mg of RH sample was placed into a ceramic pan crucible and consequently heated from 40 °C to 800 °C at three different heating rates of 5, 10, and 20 °C/min to generate data required for investigating the thermal kinetic parameters. An inert atmosphere in the pyrolysis reactor was maintained using nitrogen gas at 100 ml/min of flow rate.

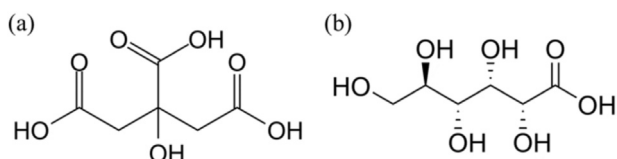


Fig. 1. Chemical structure of citric acid (a) and gluconic acid (b).

The experimental data obtained by TGA/DTA were used to calculate the kinetic parameters by employing three different iso-conversional methods: Flynn-Wall-Ozawa (FWO) model (Takeo, 1965) in Eq. (2), Kissinger-Akahira-Sunose (KAS) model (Akahira and Sunose, 1971) in Eq. (3), and Starink model (Starink, 2003) in Eq. (4). These methods were considered regarding their simplicities and excellent experimental data fitting (Kumar et al., 2020).

$$\ln(\beta) = \ln\left(\frac{AE_\alpha}{RG(\alpha)}\right) - 5.532 - 1.052\left(\frac{E_\alpha}{RT_\alpha}\right) \quad (2)$$

$$\ln\left(\frac{\beta}{T^2}\right) = \ln\left(\frac{AE_\alpha}{RG(\alpha)}\right) - \left(\frac{E_\alpha}{RT_\alpha}\right) \quad (3)$$

$$\ln\left(\frac{\beta}{T^{1.92}}\right) = \ln\left(\frac{AE_\alpha}{RG(\alpha)}\right) - 1.0008\left(\frac{E_\alpha}{RT_\alpha}\right) \quad (4)$$

Activation energies at a specific conversion rate (α) were obtained from the set of slopes of the experimental fitted line of $1/T$ against $\ln(\beta)$ (FWO), $\ln(\beta/T^2)$ (KAS), and $\ln(\beta/T^{0.92})$ (Starink).

2.4. Characterization of BSi

The inorganic species composition of the final product was determined using Inductively Coupled Plasma-Optical Emission Spectrometry (ICP-OES) (Agilent CrossLab Varian 720-ES) and X-rays Fluorescence Spectroscopy (XRF) (Thermo Niton XL5), respectively. The chosen operating conditions were: RF power 1.2 kW, plasma flow 15 L/min, auxiliary flow 1.5 L/min, nebulizer flow 0.75 L/min, sample uptake delay 30 s pump rate 15 rpm, and rinse time 10 s. The diffraction profiles of BSi were characterized using X-ray diffraction (XRD, Bruker D8 Advance) with Cu K α radiation ($\lambda = 1.5406$ Å), current voltages of 40 kV and 40 mA, scanning speed of 0.05 °C/s at $2\theta = 10$ – 90° . The silica crystals were then identified by XRD specific software (Match. Version 3). The BSi surface properties were investigated using Fourier-transform Infrared (FTIR) (Frontier MIR/FIR) coupled with Deuterated Triglycine Sulphate (DTGS) detector. The optical system with the KBr beam splitter is controlled in the range of 650–4000 cm^{-1} at a high resolution of 0.4 cm^{-1} . The Brunauer–Emmett–Teller (BET) surface area and Barrett–Joyner–Halenda (BJH) plots were obtained using a Micromeritics ASAP 2020 V3.00H system at low temperature (-196 °C) adsorption of nitrogen. Prior to measurements, the samples were degassed under low pressure for 4 h at 120 °C.

2.5. Environmental impact assessment

The environmental impacts of RH leaching during BSi production were systematically analyzed using the life cycle assessment (LCA) approach. The LCA study objective was to evaluate and compare the environmental impacts of BSi production with two different pre-treatment routes. It was carried out using open LCA software. Fig. S1 illustrates the system boundary in the present study. The system boundary of this work was a combination of ‘cradle-to-gate’ and ‘gate-to-gate’ boundaries. Since the focus of this work was to investigate the preferable methods for producing BSi, the upstream of raw material and carboxylic acids were not considered. Thus, a gate-to-gate boundary was more suitable. Otherwise, electricity and processed water utilization were critical in BSi production. Therefore, further traceback was required for those utilities. In this regard, a cradle-to-gate boundary was considered for each pathway.

The process data inputs and outputs for each system were calculated based on mass balance, as shown in Tables S2 and S3. The

wastewater from the leaching process contained acid residue and trace amounts of Si, Al, Fe, Cu, Mn, Zn, Na, Ca, and Mg. Those organic and metal components were considered as emissions to water. Wastewater from the washing process was likewise assumed as emissions to water. On the other hand, the flue gas from the calcination process was regarded as emissions to air. All electricity used for each pathway was assumed as low voltage due to simplification and conservation reasons. The emissions and losses associated with converting from high-to medium-to low-voltage electricity were available in the Agribalysev3.0.1. Meanwhile, the European Life Cycle Database (ELCDv3.2) provided the life cycle inventory data for processed water.

Tool for Reduction and Assessment of Chemicals and Other Environmental Impacts (TRACiv2.1) was used to evaluate the environmental impacts of both the leaching routes. It was included ten categories: ozone depletion (OD), global warming (GW), photochemical smog (PS), acidification (AC), eutrophication (EU), human health carcinogenic (HHC), human health non-carcinogenic (HHNC), and respiratory effects (RE), ecotoxicity (EC), and fossil fuel depletion (FFD) (Bare, 2011). The potential impact of all chemicals for the individual impact category was determined by considering their weights and characterization factors (Bare, 2011), as seen in Eq. (5).

$$I^i = \sum_{xm} CF_{xm}^i \times M_{xm} \quad (5)$$

where I^i represents the potential impact of all chemicals (x) for a particular impact category (i), denotes the characterization factor of chemical (x) emitted to media (m) for impact category (i), and M_{xm} expresses the mass of chemical (x) emitted to media (m). The characterization factor values of the emitted chemical in this work are provided in Table S4.

3. Results and discussion

3.1. Removal of metal alkali species in RH

Fig. 2 demonstrates the carboxylic acid leaching effect on removing metal alkali species. In the absence of carboxylic acids, K_2O and Na_2O were significantly decreased during the leaching process at 83.21% and 73.32%, respectively. It evidenced that K and Na were primarily water-soluble. Compared to alkali species, lower removal percentages (23.26–64.19%) were found on alkaline and metal in RH, attributed to acid-leachable behavior. Another reason could be considered regarding the distinct distribution of those metals in RH. K and Na were in the form of the unbound state at the lignocellulosic structure edge. Otherwise, the alkaline and metal species were probably bound at the inner part of the organic matter network (Chen et al., 2017).

The presence of CA or GA in the aqueous solution enhanced the removal percentage of all RH impurities. It was carried out by chelation reaction between hydroxycarboxylic sites with targeted metals to form a metal complex then discharged into solution, as shown in the following equations. The removal percentage of metal alkali impurities showed fluctuating trends as the CA or GA concentration increased. It was related to the competitive chelation reaction between reactive sites on GA or CA and multiple inorganic species in RH. The literature results also mentioned that the

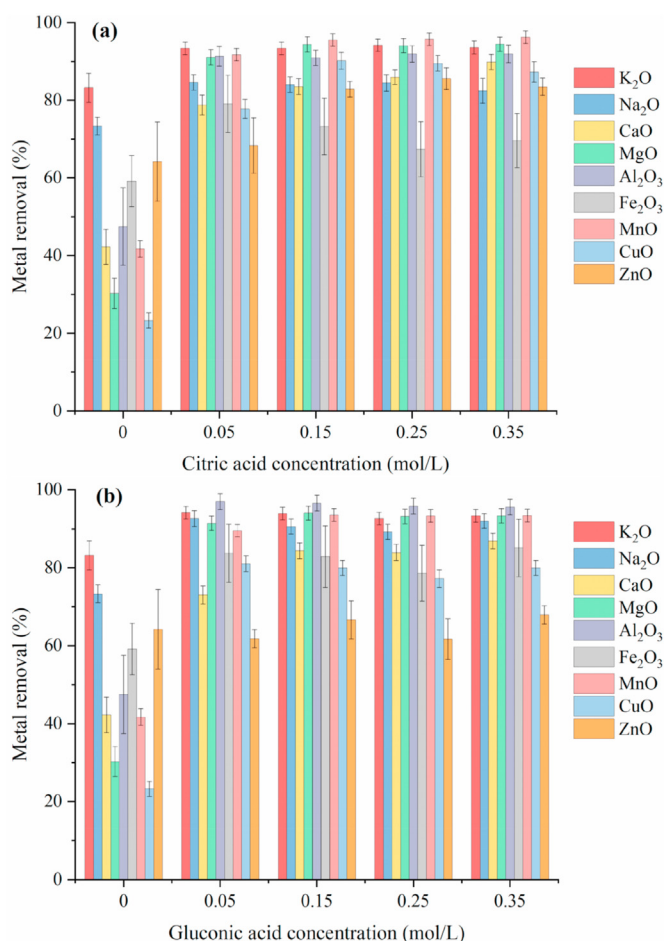
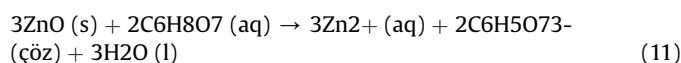
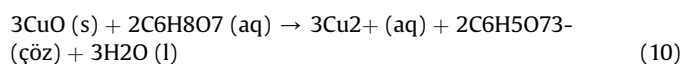
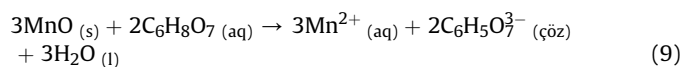
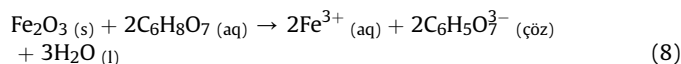
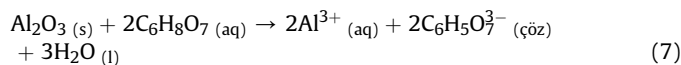
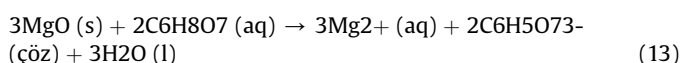
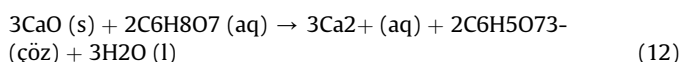


Fig. 2. RH metal alkali species removal by carboxylic acid leaching at different concentrations using citric acid (a) and gluconic acid (b).

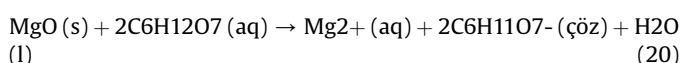
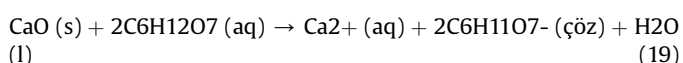
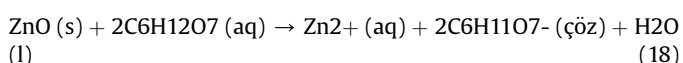
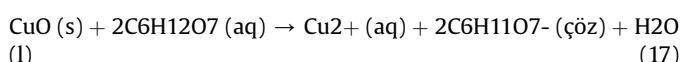
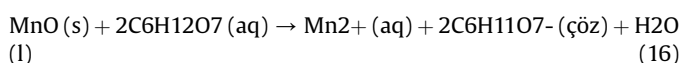
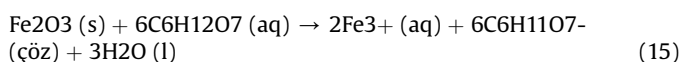
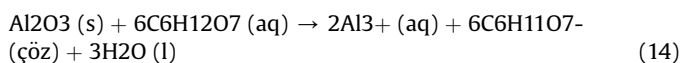
formation of saturated film layers mainly caused decreasing metal removal trends at a higher carboxylic acid concentration around particles with low solubility (Bayrak et al., 2010).

3.2.1. CA leaching reactions





3.2.2. GA leaching reactions



The carboxylic acid leaching ability was determined by the stability constant of their metal-ligand complex. It depends on the number of chelate rings, the number of donor atoms of chelating molecules, and the metal ions radius. As seen in Table S5, CA showed strong complexation with Al^{3+} , Mn^{2+} , Zn^{2+} , Ca^{2+} , and Mg^{2+} , while GA provided remarkable stability constant for Fe^{3+} and Cu^{2+} . The higher stability constant was less suitable for the RH leaching process because the metal-ligand complexes were not accessible to be protonated. Thus, GA was theoretically better than CA for removing metal impurities from RH. The results in this work exhibited some opposite trends. Both GA and CA revealed quite similar overall performances for removing metal alkali impurities of BSi in RH, as seen in Fig. 2a–b. CA provided lower solution pH than GA, reducing the stability of formed metal complex due to protonation of ligand functional groups. On the other hand, the gluconic acid structure consists of one carboxyl and four secondary hydroxyl groups (α , β , γ , δ), which could create a tridentate-complexation with trivalent metal ions (Lakatos et al., 2008) or water-soluble species (e.g., Na and K). Thus, the removal percentages of Al_2O_3 and Na_2O in GA leaching were sufficiently higher than that of CA at 95.57–97% and 89.19–92.16%, respectively.

Fig. 3a shows the pH effect on the silica discharged ratio. The silica lost during carboxylic acid leaching can be explained by considering the isoelectric point (IEP) of silica at $\text{pH} \approx 2$. At pH 6.5 without acid load, the amorphous silica would be dissolved into the water at the highest rate, 9.16%. In this condition ($\text{pH} > 2$), silica species (e.g., silicate) were negatively charged then reacted with water ion molecules to form mono silicic acid. The solution pH was gradually decreased near the silica IEP with CA or GA load, and then the negatively charged silica species was significantly dropped. At a pH around isoelectric point ($\text{IEP} \approx 2$), silica species became uncharged, slow condensation rate, and weak interactions between silicate species and ligand occurred (Wu et al., 2013). The most

negligible silica losses were achieved by 0.15 mol/L of CA ($\text{pH} 1.81$) and 0.25 mol/L of GA ($\text{pH} 1.98$) as much as 0.55% and 1.66%.

Fig. 3b shows the silica purity obtained by carboxylic acid leaching at different concentrations. Accordingly, both CA and GA exhibited relatively high silica purity. However, the silica purity (i.e. metal removal efficiency) was statistically insignificant between citric acid and gluconic acid leaching. In the presence of 0.35 mol/L CA, the silica purity could be enhanced, up to 99.14%. At the same molarity, leaching using GA exhibited slightly higher silica purity, up to 99.30%. That was due to the excellent performance of GA to remove predominant inorganic fractions in comparison with CA (see Fig. 2). The higher carboxylic acid molarity increased the silica purity, but the silica loss was unavoidable due to the pH value being lower than the IEP of silica. Thus, the carboxylic acid leaching performance on BSi recovery should be evaluated by considering the efficiency based on the amount of recovered silica and remaining RH impurities, as shown in Fig. 3c. Accordingly, the leaching efficiency was approximately 90% obtained by 0.15 mol/L of CA and 0.25 mol/L of GA, respectively. In this regard, 0.15 mol/L of CA and 0.25 mol/L of GA were both considerable to recover silica particles from RH. It also implied that GA provides a good alternative for recovering silica from RH. To further understand the BSi impurity, the chemical compositions of BSi were determined by ICP/OES and XRF, respectively (as shown in Table S6). Based on the results of BSi characteristics, the chemical compositions of RHA and BSi analyzed by XRF were similar to that determined by ICP/OES. Meanwhile, Na_2O , K_2O , CaO , MgO , Al_2O_3 , Fe_2O_3 , CuO , MnO , and ZnO were major impurities in BSi while the amounts of CdO , Cr_2O_3 , NiO , PbO_2 , As_2O_3 , HgO , Ag_2O , CoO , MoO_2 , Sb_2O_3 , SeO_2 , and V_2O_5 were negligible. In summary, the impurities of BSi obtained from CA and GA were less than 1% (as shown in Table S6) as well as the recovered silica purity was higher than 99%.

3.2. Metal alkali removal effect on the thermal degradation behavior of RH

RH sample inorganic fractions composition changes due to carboxylic acid leaching would subsequently impact their thermal decomposition behavior. It was determined by thermal kinetic analysis in the conversion (α) range of 0.1–0.9 and a temperature range of 40–800 °C. As seen in Table S7, the RH activation energies calculated by the FWO, KAS, and Starink methods were very close, indicating the accuracy of experimental fitted data. That was also confirmed by the correlation coefficients value (R^2) higher than 0.90 for all samples. Hemicellulose decomposition was characterized by the lowest activation energy of 119.54–165.96 kJ/mol at $\alpha = 0.1$ (as indicated in Table S7), located in the temperature interval 260–279 °C (as shown in Fig. S2). The conversion rates of 0.2–0.8 were attributed to cellulose decomposition, located in the temperature interval of 285–378 °C (as shown in Fig. S2), with 173–228 kJ/mol activation energies (as indicated in Table S7). Besides, relatively high activation energies around 460 kJ/mol $\alpha = 0.9$ corresponded to the charring of residue.

In general, the absence of alkali and alkaline earth metals (AAEMs) and other metal species in RH could increase the RH activation energy (Cen et al., 2019; Kim et al., 2019; Kumar et al., 2020). The results in this study, however, showed the contradictory phenomenon with lower activation energy values. As seen in Figs. S3a–c, water pre-treatment exhibited lower activation energies than untreated RH at $\alpha = 0.1$ –0.9. It was related that the loss of amorphous silica is relatively severe, with water pre-treatment at pH 6.5. The silica layers abatement on the lignocellulosic RH structure eased pyrolysis gas diffusion to contact a combustible RH fraction, resulting in lower activation energy (Zhang et al., 2020).

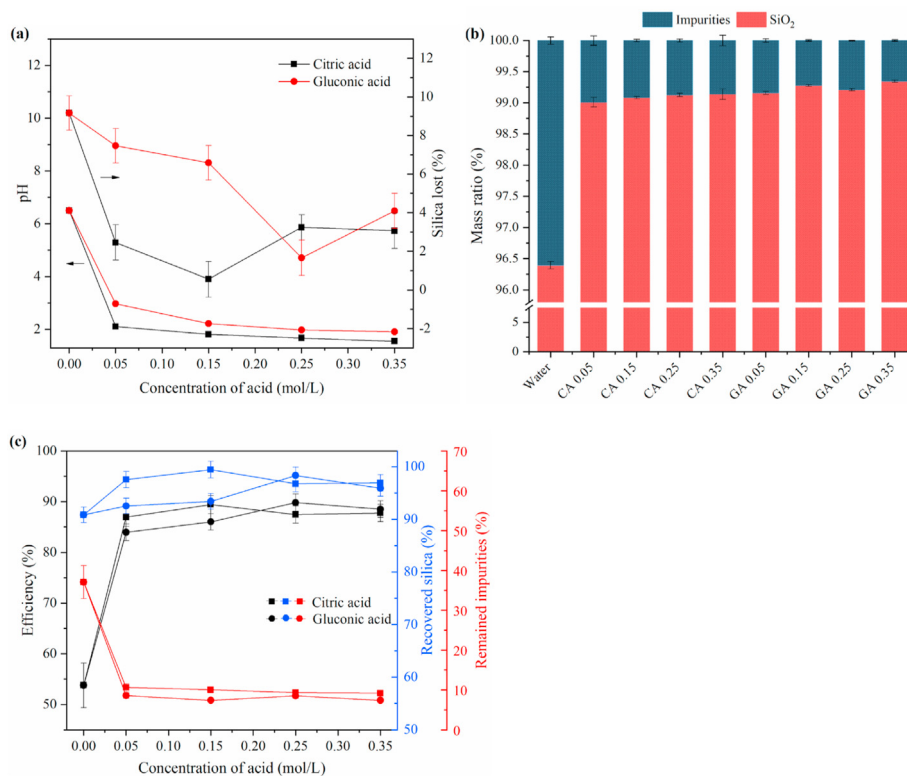


Fig. 3. Silica lost during carboxylic acid leaching (a), changes in silica purity at different carboxylic acid concentrations (b), and efficiencies of CA and GA leaching processes based on silica recovery and metal alkali removal (c).

Once the CA 0.15 mol/L was applied, the RH activation energies were initially 17–25% lowered at $\alpha = 0.1$ –0.45 (~116–177 kJ/mol), then 1–3% exceed the values of untreated RH from $\alpha = 0.5$ –0.7 (~184–187 kJ/mol). CA leaching could form smaller RH molecular monosaccharides, such as furfural and levoglucosan (Umeda and Kondoh, 2010), causing easier RH thermal degradation. The alkali metal oxides (e.g., CaO, MgO, and K₂O) and metal oxides (e.g., Al₂O₃ and Fe₂O₃) exhibited a catalytic effect on RH thermal degradation (Loy et al., 2018). Therefore, the RH activation energies would be reduced due to the absence of those oxides.

The application of GA 0.25 mol/L during the leaching process provided different RH thermal degradation effects than CA. Initially, the RH activation energies 1–5% increased, exceeding the untreated RH values. It was then slightly decreased at $\alpha = 0.3$ (~190 kJ/mol) due to the least silica abatement on the RH structure. At $\alpha = 0.4$ –0.7, the activation energies of RH with GA leaching were 2–10% higher than other RH samples (~186–200 kJ/mol). Unlike CA, GA exhibited slightly better performance on removing metal alkali impurities in RH during leaching process (see Fig. 2). Thus, the RH activation energies in many conversion rates were increased.

3.3. Characteristics of BSi

Fig. 4a illustrates the BSi FTIR spectra with different pre-treatment methods. Firm peaks at 1050–1090 cm⁻¹ and 790 cm⁻¹ indicated asymmetric vibration of Si–O–Si bond and symmetric stretching of Si–O–Si bond (Sankar et al., 2018; Shahnani et al., 2018; Azat et al., 2019). All samples showed identical SiO₂ spectra, indicating that the carboxylic acid leaching could not alter the BSi surface properties. The peaks around 3385, 1640, 2973 cm⁻¹ were attributed to stretching vibration of the O–H bond from the

silanol groups (Si–OH), bending the H–OH bond of the adsorbed water molecules (Sankar et al., 2018; Shahnani et al., 2018), and broad –OH stretching vibration, respectively. It was related to the fact that BSi was amorphous hydrated silica (SiO₂ · nH₂O). Since the dehydroxylation of surface OH groups during calcination of RH at 800 °C was reversible, the silica surface will be physically covered by adsorbed water (multiple layers of H₂O) during temperature cooling down to room temperature.

XRD patterns of BSi samples are illustrated in Fig. 4b. Untreated BSi showed three crystalline phases of silica: cristobalite ($2\theta = 22^\circ$, 28.47° , 31.45° , and 36.22°), quartz- α -SiO₂ ($2\theta = 20.86^\circ$), and quartz ($2\theta = 27.67^\circ$). Although the combustion process was operated below the silica melting point at 1000 °C, crystallization of amorphous BSi could not be avoided. Alkali components in RH (Na and K) might have a eutectic reaction with silica to form ternary oxides (e.g., Na₆Si₈O₁₉ and Na₂Si₂O₅), resulting in a dramatic decrement of silica melting point at around 800 °C. After solidifying ternary oxides, the massive amounts of amorphous BSi would be transformed into a crystalline phase. The crystalline silica phases disappeared after carboxylic acid leaching, confirmed by the broad peak at $2\theta = 22^\circ$, as shown in Fig. 4b. It indicated that sufficient alkali removal by both CA and GA leaching processes could maintain the original phase of BSi. This amorphous structure should be controlled to avoid the carcinogenic effect of crystalline silica dust, causing lung cancer (Borm et al., 2011).

All BSi samples exhibited type IV isotherms typical for mesoporous materials, as shown in Fig. 4c. The isotherms of untreated BSi showed a type H4 hysteresis loops at P/P₀ = 0.14–0.99, associated with narrow slit pores. Meanwhile, N₂ physisorption isotherms of BSi pre-treated by CA, GA, or water showed the type of H3 hysteresis loops at P/P₀ = 0.4–0.99 typically observed in the particulate aggregates having irregular slit-shaped pores. Metal

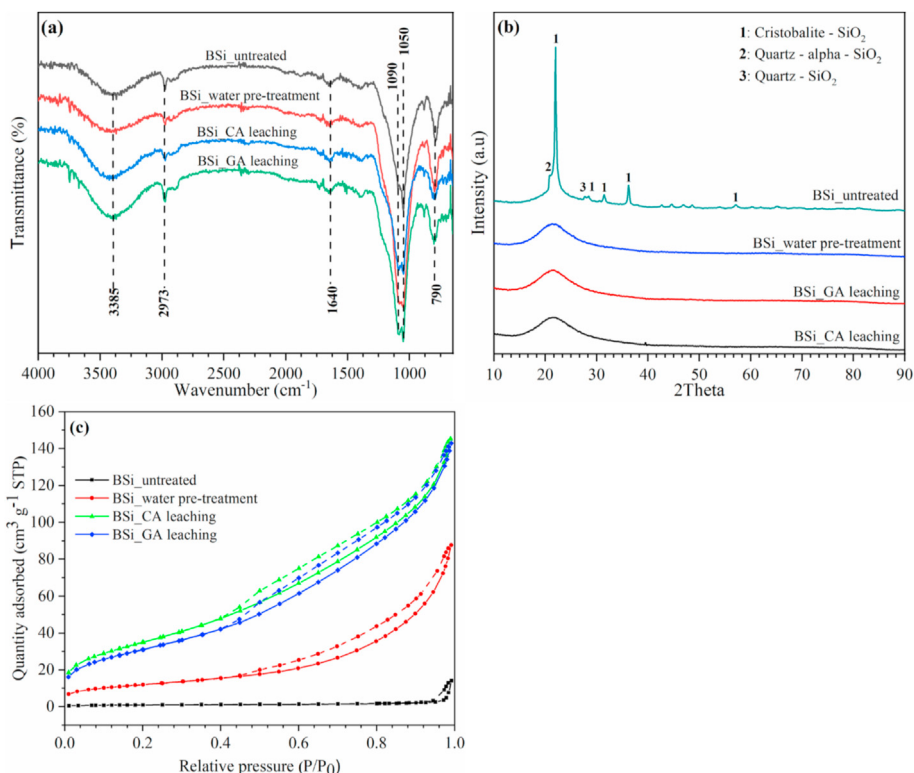


Fig. 4. Physicochemical characterization results of BSi: FTIR spectra (a), XRD profiles (b), and N₂ physisorption isotherms (c).

Table 2

Textural properties of BSi with different pre-treatment.

Pre-treatment	Pore size (nm)	Specific surface area (m ² /g)	Pore volume (cm ³ /g)
Untreated	35.30	2.95	0.02
Water	11.25	43.41	0.14
Citric acid	6.25	128.43	0.23
Gluconic acid	6.70	114.06	0.23

alkali impurities were embedded on the surface of amorphous silica particles. Various metal species were reduced during carboxylic acid leaching, then the intermolecular contact among silica particles could be intensified to form solemn aggregation with a different narrow slit.

Fig. S4 shows pore size distributions (PSD) calculated by the Barrett-Joyner-Halenda (BJH) model. All samples exhibited unimodal distribution with the main pore sizes of ~11.50 nm, ~6.25 nm, and ~6.70 nm for treated BSi with water, CA, and GA. These values proved the above-mentioned findings regarding BSi pore shapes.

On the other hand, the different BSi pore size values prepared by water, CA, or GA pre-treatment were possibly correlated to the amount of discharged silica into the solution during the operation process. A higher amount of dissolved silica left more irregular voids on the silica particle surface. Therefore, this tendency was well-matched with the pore size of RH (water > GA > CA). Table 2 summarizes the textural properties of BSi samples. The specific surface area and pore volume of untreated BSi were shallow at 2.95 m²/g and 0.02 cm³/g, respectively. The crystallization process was responsible to reduces surface area and total void volumes (Bie

Table 3

Results of ten impact categories of the two BSi production pathways.

Impact category	Unit	BSi (GA leaching)	BSi (CA leaching)
Eutrophication (EU)	kg N eq	0.02	0.02
Fossil fuel depletion (FFD)	MJ surplus	1.03	1.03
Global warming (GW)	kg CO ₂ eq	3.57	3.57
Acidification (AC)	kg SO ₂ eq	0.02	0.02
Respiratory effects (RE)	kg PM _{2.5} eq	0.002	0.002
Carcinogenic (HHC)	CTUh	2.77 × 10 ⁻⁷	2.77 × 10 ⁻⁷
Non carcinogenic (HHNC)	CTUh	1.36 × 10 ⁻⁶	1.37 × 10 ⁻⁶
Ozone depletion (OD)	kg CFC-11 eq	2.73 × 10 ⁻⁷	2.73 × 10 ⁻⁷
Ecotoxicity (EC)	CTUe	35.42	46.92
Smog formation (PS)	kg O ₃ eq	0.10	0.10

et al., 2015; Fernandes et al., 2017). The carboxylic acid leaching could maintain the amorphous nature of BSi, resulting in higher surface area and pore volume.

3.4. Environmental impact assessment

The life cycle assessment results for GA leaching and CA leaching pathways are shown in Table 3. Since the utilization of electricity and processed water during GA leaching was identical to CA leaching, most impact categories (EU, FFD, GW, AC, RE, OD, and PS) exhibited similar values. GA leaching showed lower HHNC and EC than CA leaching at 1.36×10^{-6} CTU_h (Comparative Toxic Units to Humans) and 35.42 CTU_e (Comparative Toxic Units to Ecotoxicity), respectively. It was due to less amount of Zn and Cu, which could be removed from BSi during the leaching process. Likewise, the environmental impact of GA residue was not considered in TRA-CIV2.1, contributing to a lower amount of EC. That was probably related to the excellent biodegradability of GA, 98% at two days (Ramachandran et al., 2006).

Fig. S5a shows the percentage contribution of various processes to the overall environmental impacts of the CA leaching route. The calcination process provided a predominant contribution to all environmental impact categories except EC. The highest contribution in EC, 46.76%, was exhibited by the leaching process. Wastewater containing CA residue and dissolved metal components (Zn and Cu) was responsible for the higher EC impact result. GA leaching reduced the leaching process contribution to EC by 27.51% (see Fig. S5b). It was again related to the superior biodegradability of GA and less amount of removed Zn and Cu during leaching process.

4. Conclusions

The performances of biogenic silica (BSi) prepared from rice husk by carboxylic acid leaching has been successfully evaluated as well as the environmental impact by life cycle assessment (LCA). Meanwhile, gluconic acid (GA) was proposed in rice husk pretreatment for the first time during BSi production and compared its performance with citric acid (CA) as a common carboxylic acid. The results indicated that both GA and CA had sufficient capacity to remove major metal alkali impurities in RH with a few silica losses. In GA, polyhydroxy groups were evidently beneficial to provide an additional reaction site instead of the carboxyl group during the leaching process. Lower RH thermal degradation activation energies were caused mainly by the combined effect of silica loss and high removal impurities. Both GA and CA could produce high-purity BSi with identical properties, primarily mesoporous with lower specific surface area and pore volume. LCA results indicated that the GA leaching exhibited a minor contribution to all environmental impact categories. The present study gives insight that GA is an excellent and new eco-friendly carboxylic acid for producing BSi from RH.

Credit author statement

Wahyu Kamal Setiawan: Conceptualization; Methodology; Formal analysis; Writing – original draft; Writing – review & editing. **Kung-Yuh Chiang:** Technically supporting; Reviewing and revising; Supervising.

Declaration of competing interest

The authors declare that they have no known competing financial interests or personal relationships that could have influenced the work reported in this paper.

Acknowledgments

The authors would like to thank the Taiwan Ministry of Science and Technology (MOST) (MOST-108-2221-E-008-061) for financially supporting this work. The authors also would like to thanks the Precision Instrument Support Center of National Central University in providing the analysis facilities.

Appendix A. Supplementary data

Supplementary data to this article can be found online at <https://doi.org/10.1016/j.chemosphere.2021.130541>.

References

- Akshira, T., Sunose, T., 1971. Method of determining activation deterioration constant of electrical insulating materials. Res. Rep. Chiba Inst. Technol. (Sci. Technol.) 16, 22–31.
- Alyosef, H.A., Eilert, A., Welscher, J., Ibrahim, S.S., Denecke, R., Schwiager, W., Enke, D., 2013. Characterization of biogenic silica generated by thermo chemical treatment of rice husk. Part. Sci. Technol. 31, 524–532.
- Azat, S., Korobeinyk, A.V., Moustakas, K., Inglezakis, V.J., 2019. Sustainable production of pure silica from rice husk waste in Kazakhstan. J. Clean. Prod. 217, 352–359.
- Bach, Q.-V., Vu, C.M., Vu, H.T., Nguyen, D.D., 2019. Enhancing mode I and II inter-laminar fracture toughness of carbon fiber-filled epoxy-based composites using both rice husk silica and silk fibroin electrospun nanofibers. High Perform. Polym. 31, 1195–1203.
- Bakar, R.A., Yahya, R., Gan, S.N., 2016. Production of high purity amorphous silica from rice husk. Procedia Chem. 19, 189–195.
- Bare, J., 2011. TRACI 2.0: the tool for the reduction and assessment of chemical and other environmental impacts 2.0. Clean Technol. Environ. Policy 13, 687–696.
- Bayrak, B., Laçın, O., Saraç, H., 2010. Kinetic study on the leaching of calcined magnesite in gluconic acid solutions. J. Ind. Eng. Chem. 16, 479–484.
- Beidaghy Dizaji, H., Zeng, T., Hartmann, I., Enke, D., Schliermann, T., Lenz, V., Bidabadi, M., 2019. Generation of high quality biogenic silica by combustion of rice husk and rice straw combined with pre- and post-treatment strategies—a review. Appl. Sci. 9.
- Bie, R.-S., Song, X.-F., Liu, Q.-Q., Ji, X.-Y., Chen, P., 2015. Studies on effects of burning conditions and rice husk ash (RHA) blending amount on the mechanical behavior of cement. Cement Concr. Compos. 55, 162–168.
- Borm, P.J., Tran, L., Donaldson, K., 2011. The carcinogenic action of crystalline silica: a review of the evidence supporting secondary inflammation-driven genotoxicity as a principal mechanism. Crit. Rev. Toxicol. 41, 756–770.
- Cañete-Rodríguez, A.M., Santos-Dueñas, I.M., Jiménez-Hornero, J.E., Ehrenreich, A., Liebl, W., García-García, I., 2016. Gluconic acid: properties, production methods and applications—an excellent opportunity for agro-industrial by-products and waste bio-valorization. Process Biochem. 51, 1891–1903.
- Cen, K., Zhang, J., Ma, Z., Chen, D., Zhou, J., Ma, H., 2019. Investigation of the relevance of biomass pyrolysis polygeneration and washing pretreatment under different severities: water, dilute acid solution and aqueous phase bio-oil. Bioresour. Technol. 278, 26–33.
- Chen, P., Gu, W., Fang, W., Ji, X., Bie, R., 2017. Removal of metal impurities in rice husk and characterization of rice husk ash under simplified acid pretreatment process. Environ. Prog. Sustain. Energy 36, 830–837.
- Davarpanah, J., Sayahi, M.H., Ghahremani, M., Karkhoie, S., 2019. Synthesis and characterization of nano acid catalyst derived from rice husk silica and its application for the synthesis of 3,4-dihydropyrimidinones/thiones compounds. J. Mol. Struct. 1181, 546–555.
- Dhinasekaran, D., Raj, R., Rajendran, A.R., Purushothaman, B., Subramanian, B., Prakasarao, A., Singaravelu, G., 2020. Chitosan mediated 5-Fluorouracil functionalized silica nanoparticle from rice husk for anticancer activity. Int. J. Biol. Macromol. 156, 969–980.
- Duan, D., Ruan, R., Wang, Y., Liu, Y., Dai, L., Zhao, Y., Zhou, Y., Wu, Q., 2018. Microwave-assisted acid pretreatment of alkali lignin: effect on characteristics and pyrolysis behavior. Bioresour. Technol. 251, 57–62.
- Fernandes, I., Lucca Sánchez, F., Jurado, J., Kieling, A., Rocha, T., Moraes, C.A., Sousa, V., 2017. Physical, chemical and electric characterization of thermally treated rice husk ash and its potential application as ceramic raw material. Advanced Powder Technology.
- Gomes, C.M., Garry, A.-L., Freitas, E., Bertoldo, C., Siqueira, G., 2020. Effects of rice husk silica on microstructure and mechanical properties of magnesium-oxychloride fiber cement (MOFC). Construct. Build. Mater. 241, 118022.
- Goodman, B.A., 2020. Utilization of waste straw and husks from rice production: a review. J. Bioresour. Bioprod. 5, 143–162.
- Jyoti, A., Singh, R.K., Kumar, N., Aman, A.K., Kar, M., 2021. Synthesis and properties of amorphous nanosilica from rice husk and its composites. Mater. Sci. Eng., B 263, 114871.
- Karwowska, B., 2012. Optimization of metals ions extraction from industrial wastewater sludge with chelating agents/optymalizacja procesu ekstrakcji

- jonów metali Z przemysłowych osadów sciekowych za pomocą roztworów związków chelatujących. *Arch. Environ. Protect.* 38.
- Kim, K.H., Jeong, K., Kim, S.-S., Brown, R.C., 2019. Kinetic understanding of the effect of Na and Mg on pyrolytic behavior of lignin using a distributed activation energy model and density functional theory modeling. *Green Chem.* 21, 1099–1107.
- Kumar, M., Mishra, P.K., Upadhyay, S.N., 2020. Thermal degradation of rice husk: effect of pre-treatment on kinetic and thermodynamic parameters. *Fuel* 268, 117164.
- Lakatos, A., Kiss, T., Bertani, R., Venzo, A., Di Marco, V.B., 2008. Complexes of Al(III) with d-gluconic acid. *Polyhedron* 27, 118–124.
- Lee, J.H., Kwon, J.H., Lee, J.-W., Lee, H.-s., Chang, J.H., Sang, B.-I., 2017. Preparation of high purity silica originated from rice husks by chemically removing metallic impurities. *J. Ind. Eng. Chem.* 50, 79–85.
- Lei, C., Li, Z., Gao, Q., Fu, R., Wang, W., Li, Q., Liu, Z., 2020. Comparative study on the production of gluconic acid by electro dialysis and bipolar membrane electro dialysis: effects of cell configurations. *J. Membr. Sci.* 608, 118192.
- Loy, A.C.M., Gan, D.K.W., Yusup, S., Chin, B.L.F., Lam, M.K., Shahbaz, M., Unrean, P., Acda, M.N., Rianawati, E., 2018. Thermogravimetric kinetic modelling of in-situ catalytic pyrolytic conversion of rice husk to bioenergy using rice hull ash catalyst. *Bioresour. Technol.* 261, 213–222.
- Martínez, A., Vargas, R., Galano, A., 2018. Citric acid: a promising copper scavenger. *Computat. Theor. Chem.* 1133, 47–50.
- Mathur, L., Saddam Hossain, S.K., Majhi, M.R., Roy, P.K., 2018. Synthesis of nanocrystalline forsterite (Mg₂SiO₄) powder from biomass rice husk silica by solid-state route. *Bol. Soc. Espanola Ceram. Vidr.* 57, 112–118.
- Pal, P., Kumar, R., Banerjee, S., 2016. Manufacture of gluconic acid: a review towards process intensification for green production. *Chem. Eng. Process: Process Intensific.* 104, 160–171.
- Pham, T.D., Bui, T.T., Trang Truong, T.T., Hoang, T.H., Le, T.S., Duong, V.D., Yamaguchi, A., Kobayashi, M., Adachi, Y., 2020a. Adsorption characteristics of beta-lactam cefixime onto nanosilica fabricated from rice HUSK with surface modification by polyelectrolyte. *J. Mol. Liq.* 298, 111981.
- Pham, T.D., Vu, C.M., Choi, H.J., 2017. Enhanced fracture toughness and mechanical properties of epoxy resin with rice husk-based nano-silica. *Polym. Sci.* 59, 437–444.
- Pham, T.D., Vu, T.N., Nguyen, H.L., Le, P.H.P., Hoang, T.S., 2020b. Adsorptive removal of antibiotic ciprofloxacin from aqueous solution using protein-modified nanosilica. *Polymers* 12, 57.
- Ramachandran, S., Fontanille, P., Pandey, A., Larroche, C., 2006. Gluconic acid: properties, applications and microbial production. *Food Technol. Biotechnol.* 44.
- Sankar, S., Kaur, N., Lee, S., Kim, D.Y., 2018. Rapid sonochemical synthesis of spherical silica nanoparticles derived from brown rice husk. *Ceram. Int.* 44, 8720–8724.
- Schneider, D., Wassersleben, S., Weiß, M., Denecke, R., Stark, A., Enke, D., 2020. A generalized procedure for the production of high-grade, porous biogenic silica. *Waste Biomass Valor.* 11, 1–15.
- Setiawan, W.K., Chiang, K.-Y., 2020. Crop Residues as Potential Sustainable Precursors for Developing Silica Materials: A Review. *Waste and Biomass Valorization*.
- Shahnani, M., Mohebbi, M., Mehdi, A., Ghassempour, A., Aboul-Enein, H.Y., 2018. Silica microspheres from rice husk: a good opportunity for chromatography stationary phase. *Ind. Crop. Prod.* 121, 236–240.
- Starink, M.J., 2003. The determination of activation energy from linear heating rate experiments: a comparison of the accuracy of isoconversion methods. *Thermochim. Acta* 404, 163–176.
- Su, Y., Liu, L., Zhang, S., Xu, D., Du, H., Cheng, Y., Wang, Z., Xiong, Y., 2020. A green route for pyrolysis poly-generation of typical high ash biomass, rice husk: effects on simultaneous production of carbonic oxide-rich syngas, phenol-abundant bio-oil, high-adsorption porous carbon and amorphous silicon dioxide. *Bioresour. Technol.* 295, 122243.
- Takeo, O., 1965. A new method of analyzing thermogravimetric data. *Bull. Chem. Soc. Jpn.* 38, 1881–1886.
- Umeda, J., Kondoh, K., 2010. High-purification of amorphous silica originated from rice husks by combination of polysaccharide hydrolysis and metallic impurities removal. *Ind. Crop. Prod.* 32, 539–544.
- Vandenbergh, L.P.S., Rodrigues, C., de Carvalho, J.C., Medeiros, A.B.P., Socol, C.R., 2017. 25 - production and application of citric acid. In: Pandey, A., Negi, S., Socol, C.R. (Eds.), *Current Developments in Biotechnology and Bioengineering*. Elsevier, pp. 557–575.
- Vu, C.M., Bach, Q.-V., Vu, H.T., Nguyen, D.D., Kien, B.X., Chang, S.W., 2020a. Carbon-Fiber-reinforced epoxy resin with sustainable additives from silk and rice husks for improved mode-I and mode-II interlaminar fracture toughness. *Macromol. Res.* 28, 33–41.
- Vu, C.M., Nguyen, V.-H., Bach, Q.-V., 2020b. Phosphorous-jointed epoxidized soybean oil and rice husk-based silica as the novel additives for improvement mechanical and flame retardant of epoxy resin. *J. Fire Sci.* 38, 3–27.
- Wang, J., Cui, Z., Li, Y., Cao, L., Lu, Z., 2020. Techno-economic analysis and environmental impact assessment of citric acid production through different recovery methods. *J. Clean. Prod.* 249, 119315.
- Wu, S.-H., Mou, C.-Y., Lin, H.-P., 2013. Synthesis of mesoporous silica nanoparticles. *Chem. Soc. Rev.* 42, 3862–3875.
- Xia, L., Hart, B., Douglas, K., 2015. The role of citric acid in the flotation separation of rare earth from the silicates. *Miner. Eng.* 74, 123–129.
- Xu, W., Wei, J., Chen, J., Zhang, B., Xu, P., Ren, J., Yu, Q., 2018. Comparative study of water-leaching and acid-leaching pretreatment on the thermal stability and reactivity of biomass silica for viability as a pozzolanic additive in cement. *Materials* 11.
- Zhang, S., Su, Y., Xu, D., Zhu, S., Zhang, H., Liu, X., 2018. Effects of torrefaction and organic-acid leaching pretreatment on the pyrolysis behavior of rice husk. *Energy* 149, 804–813.
- Zhang, Z., Wang, Q., Li, L., Xu, G., 2020. Pyrolysis characteristics, kinetics and evolved volatiles determination of rice-husk-based distiller's grains. *Biomass Bioenergy* 135, 105525.